

Relativistic calculation of pair-production positron energy-angle distributions for low-energy photons on atoms

H. K. Tseng

Department of Physics, National Central University, Chung-Li, Taiwan 32054, Republic of China

(Received 21 November 1994)

We calculated numerically in a relativistic partial-wave formulation the positron energy-angle distributions of pair production in the fields of atoms with atomic number $Z=1, 6, 13$, and 82 for photons of energies near threshold, $k=2.001, 2.01$, and $2.10m_e c^2$. Our partial-wave results show that in this low photon energy region, the atomic-electron screening effect for the positron energy-angle distributions increases as Z increases, k decreases, and the positron energy E_+ decreases. The ratio of the screened to the point-Coulomb positron energy-angle cross section is almost independent of the positron angle. That is, the shape of positron energy-angle distributions is almost independent of the screening. This suggests that the screening is primarily a normalization effect. Our results also indicate that the Born approximation prediction for the shape of positron energy-angle distributions is better than its prediction for positron energy spectra of pair production. The form of the Born approximation suggests a simple way to parametrize the shape of positron energy-angle distributions.

PACS number(s): 32.80.Cy, 32.90.+a

I. INTRODUCTION

With the continuing improvements in computational capabilities it is becoming feasible to make fairly accurate theoretical calculations of pair-production positron energy spectra by photons on atoms [1–4]. This has coincided with the need for such results in fields such as radiation physics [5]. Pair production, scattering, and photoeffect are the three processes primarily responsible for the attenuation of electromagnetic radiation in matter. For a given element the pair production dominates at high photon energies. However, from a physical point of view, results of pair-production cross sections that are differential in positron energy and positron angle provide more detailed information on the pair-production process. In this paper we wish to report predictions for the shapes of pair-production cross sections that are differential in positron energy and positron angle, to supplement our previous work [4] on the positron energy spectra of pair production for photons of energies k from $2.10m_e c^2$ down to $2.001m_e c^2$. In this work, our results are obtained with direct numerical calculations by using an exact relativistic partial-wave formulation [4]. We describe our basic process as a single-photon production of electron-positron pairs from an unpolarized isolated atom. In addition, we use a simplified model that is adequate for a wide range of atoms and the process at the kinetic energy of the created electron (or positron) above the keV range [6]. The target atom is described by a central potential [6], such as the Hartree-Fock-Slater potential with the exchange term omitted [7]. Previously [2] we had used the Kohn-Sham potential [8], which includes an approximate exchange term that is actually not appropriate for positrons [3]. Of course, as the photon energy decreases and the kinetic energy of the created elec-

tron (or positron) becomes very low, the calculations based on this independent-particle model cease to be quantitative and provide only a qualitative guide to features.

In Sec. II, we present and analyze our results for the shape function S of the pair-production cross section, differential in positron energy E_+ and positron angle θ_+ , using the results obtained from the partial-wave method [4]. This shape function is defined as the ratio of the un-

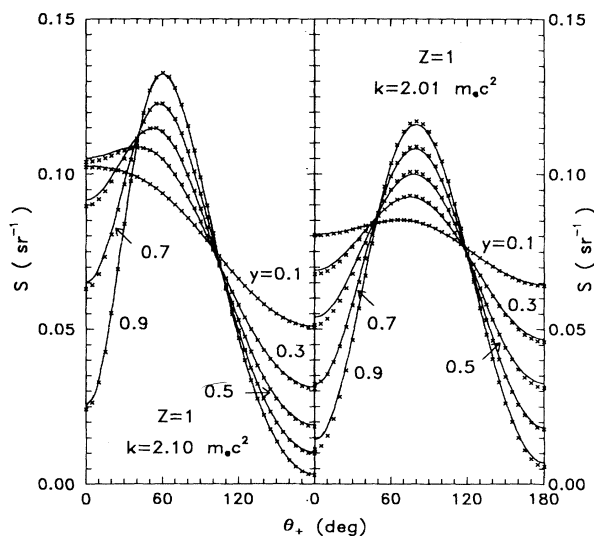


FIG. 1. Comparisons of the shape functions $S = \sigma(E_+, \theta_+)/\sigma(E_+)$ for $Z=1$, $k=2.10$ and $2.01m_e c^2$, and the point-Coulomb potential between the results obtained by the partial-wave method using Eqs. (21) and (23) of Ref. [4] (solid lines) and the results obtained by the Born approximation (the crosses).

polarized pair-production positron energy-angle cross section $\sigma(E_+, \theta_+) = [Z^{-2} d\sigma/dE_+ d\Omega_+]_{\text{unpol}}$ to the unpolarized pair-production positron energy spectrum $\sigma(E_+) = [Z^{-2} d\sigma/dE_+]_{\text{unpol}}$. Finally, we discuss how best to represent the shape functions.

II. RESULTS AND DISCUSSION

With the partial-wave method using Eqs. (21) and (23) of Ref. [4] we have obtained the shape function of pair production $S = \sigma(E_+, \theta_+)/\sigma(E_+)$ for incident photons of energies $k = 2.001, 2.01, \text{ and } 2.10 m_e c^2$, for the elements of atomic number $Z = 1, 6, 13, \text{ and } 82$. These calculated results are shown in Figs. 1–7. Here the unpolarized pair-production cross sections are calculated numerically, both with the Hartree-Fock-Slater potential with the exchange term omitted [7] (HFN potential, here N stands for no exchange term) and the point-Coulomb potential. In Figs. 1 and 2 we make comparisons of the shape functions S calculated by the numerical partial-wave method for the point-Coulomb potential with the results calculated by the Born approximation [1,9]. We see that the Born approximation prediction for the shape function is better than its prediction for the positron energy spectrum of pair production. We may understand this feature qualitatively by the following argument. In the Born approximation the shape function has the form, independent of Z ,

$$S_B = (4\pi M \Delta_+)^{-1} \left[\frac{4(2E_+^2 + 1)\sin^2\theta_+}{p_+^2 \Delta_+^3} - \frac{5E_+^2 - 2E_+ E_- + 3}{p_+^2 \Delta_+} - \frac{p_+^2 - k^2}{Q^2 \Delta_+} - \frac{2E_-}{p_+^2} \right. \\ \left. - \frac{L}{p_+ p_-} \left[\frac{2E_+(3k + p_+^2 E_-)\sin^2\theta_+}{p_+^2 \Delta_+^3} + \frac{k(E_+^2 - E_+ E_- - 1)}{p_+^2} \right. \right. \\ \left. \left. + \frac{2E_+^2(E_+^2 + E_-^2) - (7E_+^2 + 3E_+ E_- + E_-^2) + 1}{p_+^2 \Delta_+} \right] + \frac{2}{p_-} \ln \frac{E_- + p_-}{E_- - p_-} \right. \\ \left. + \frac{\ln(Q + p_-)/(Q - p_-)}{p_- Q} \left[\frac{2}{\Delta_+} - 3k - \frac{k(p_+^2 - k^2)}{Q^2} \right] \right], \quad (1)$$

where

$$M = \frac{4}{3} + \frac{2E_+ E_- (p_+^2 + p_-^2)}{p_+^2 p_-^2} - \frac{E_+ \epsilon_-}{p_-^3} - \frac{E_- \epsilon_+}{p_+^3} - \frac{\epsilon_+ \epsilon_-}{p_+ p_-} \\ - L \left[\frac{k^2}{p_+^3 p_-^3} (E_+^2 E_-^2 + p_+^2 p_-^2) - \frac{8}{3} \frac{E_+ E_-}{p_+ p_-} - \frac{k}{2p_+ p_-} \left[\frac{E_+ E_- - p_-^2}{p_-^3} \epsilon_- - \frac{E_+ E_- - p_+^2}{p_+^3} \epsilon_+ + \frac{2kE_+ E_-}{p_+^2 p_-^2} \right] \right],$$

$$L = 2 \ln \frac{E_+ E_- + p_+ p_- + 1}{k},$$

$$\epsilon_+ = 2 \ln(E_+ + p_+),$$

$$\epsilon_- = 2 \ln(E_- + p_-),$$

$$\Delta_+ = E_+ (1 - \beta_+ \cos\theta_+),$$

$$Q = \sqrt{p_+^2 + k^2 - 2p_+ k \cos\theta_+},$$

$$\beta_+ = \frac{p_+}{E_+}.$$

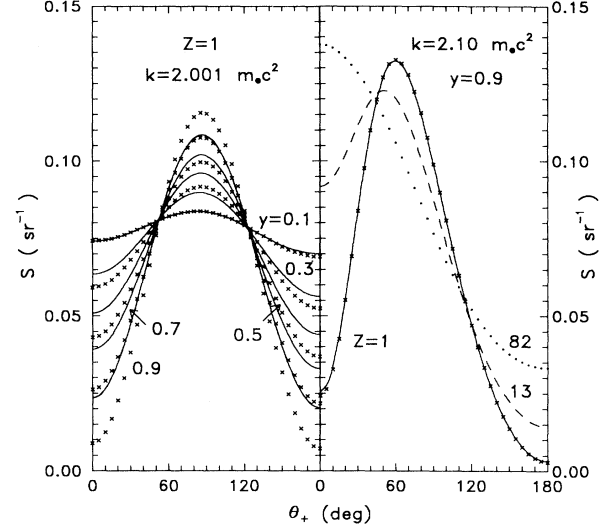


FIG. 2. Comparisons of the shape functions S for $Z=1$, $k=2.001 m_e c^2$, and the point-Coulomb potential between the results obtained by the partial-wave method using Eqs. (21) and (23) of Ref. [4] (solid lines) and the results obtained by the Born approximation (the crosses). For the right-hand panel of the figure, we show comparisons of the shape functions S for $Z=1, 13, 82$, $k=2.10 m_e c^2$, $y=(E_+ - 1)/(k - 2) = 0.9$ between the results obtained by the partial-wave method and the results obtained by the Born approximation (the crosses). Our partial-wave results for $Z=1, 13, 82$ are shown by solid line, dashed lines, and solid circles, respectively.

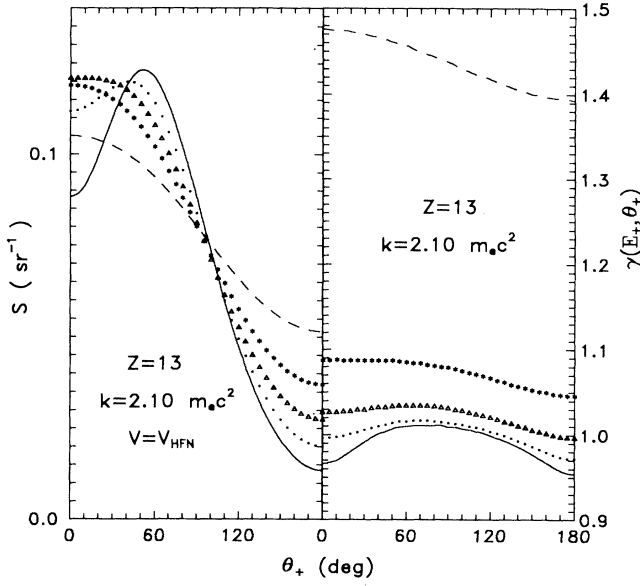


FIG. 3. Pair-production shape functions S and screening factors $\gamma(E_+, \theta_+)$ calculated by the numerical calculation in partial waves using Eqs. (21) and (23) of Ref. [4] for $Z=13$, $k=2.10m_e c^2$. The symbol V_{HFN} refers to the Hartree-Fock-Slater potential with the exchange term omitted. The results for $y=(E_+-1)/(k-2)=0.1, 0.3, 0.5, 0.7$, and 0.9 are shown by dashed lines, asterisks, empty triangles, solid circles, and solid lines, respectively.

Nishina, Tomonaga, and Sakata [1,10] found that for low energies and small values of Z , there is a simple way to improve the Born approximation prediction with a multiplicative factor,

$$\frac{2\pi\nu_+2\pi\nu_-}{(e^{2\pi\nu_+}-1)(1-e^{-2\pi\nu_-})} \left[1 + 2\pi \frac{3(\pi^2+8)}{64(k-2)} (Z\alpha)^2 \right],$$

where $\nu_{\pm}=Z\alpha/\beta_{\pm}$ and $\beta_{\pm}=p_{\pm}/E_{\pm}$. However, such a

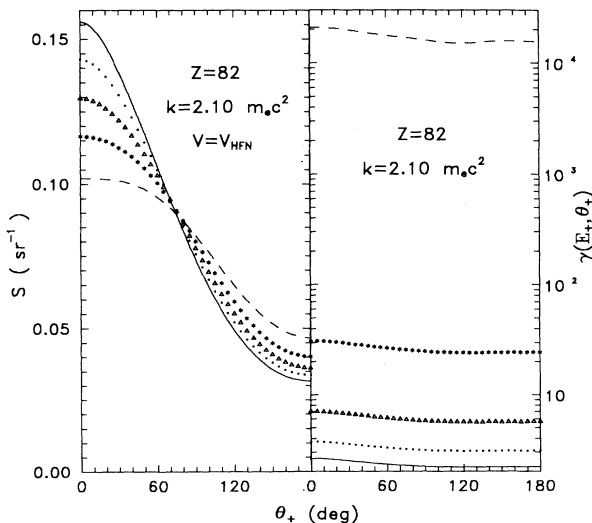


FIG. 4. Same as Fig. 3, except for $Z=82$, $k=2.10m_e c^2$.

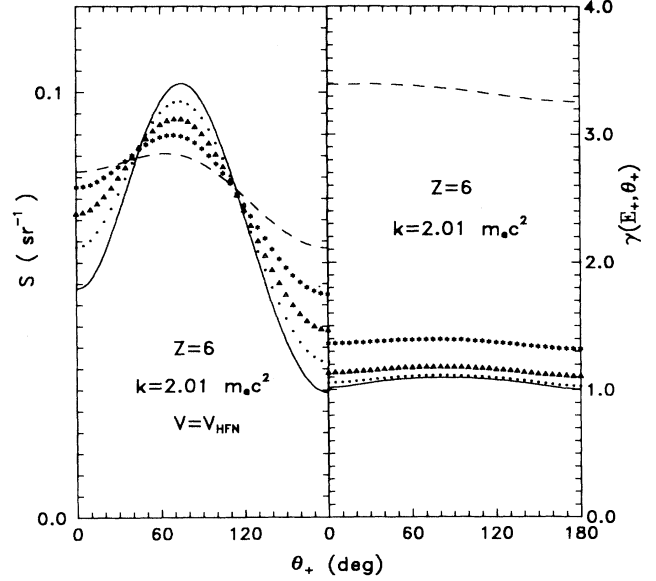


FIG. 5. Same as Fig. 3, except for $Z=6$, $k=2.01m_e c^2$.

modification, since it is independent of the angle, has no effect on the Born approximation prediction for the shape function.

In Figs. 3–7, we show the pair-production shape function S for the HFN potential and the corresponding screening factor $\gamma(E_+, \theta_+)$; the ratio of screened to point-Coulomb positron energy-angle cross sections $\sigma(E_+, \theta_+)$ calculated in partial waves for $Z=6, 13$, and 82 ; and $k=2.10, 2.01$, and $2.001m_e c^2$. Our partial-wave results show that the atomic-electron screening effect for the pair-production positron energy-angle cross section increases as Z increases, k decreases, and E_+ decreases, just like the screening effect for the pair-production ener-

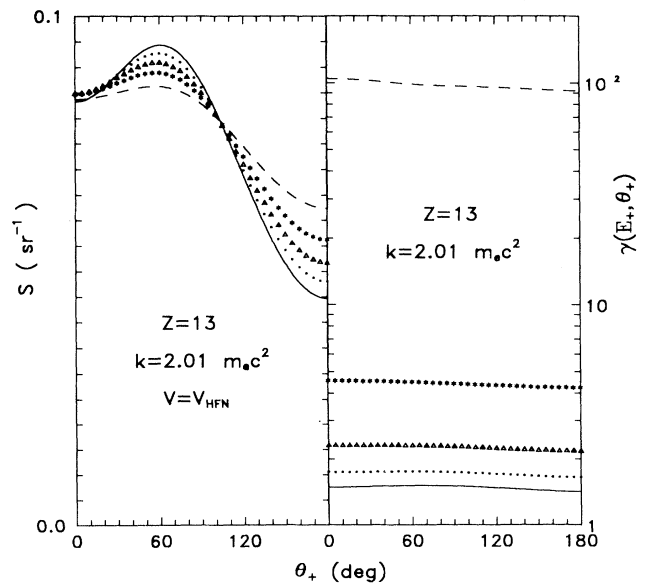


FIG. 6. Same as Fig. 3, except for $Z=13$, $k=2.01m_e c^2$.

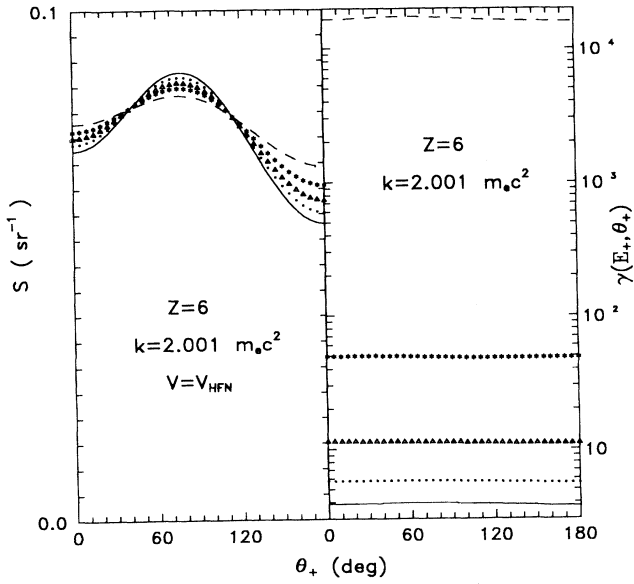


FIG. 7. Same as Fig. 3, except for $Z=6$, $k=2.001m_e c^2$.

gy spectrum. The ratio of the screened to the point-Coulomb positron energy-angle cross section is almost independent of the positron angle. That is, the shape of positron energy-angle distributions is almost independent of the screening. This suggests that the atomic-electron screening is primarily a normalization effect for the cases we consider in this paper [11].

It is desirable to identify a small number of parameters that characterize the pair-production positron energy-angle cross section $\sigma(E_+, \theta_+)$. The form of the Born approximation suggests a representation such as

TABLE I. Coefficients B_n of the shape functions S in Eq. (2) with $m=0-4$, calculated from results of the shape functions obtained by the partial-wave method using Eqs. (21) and (23) of Ref. [4] for $Z=82$, $=2.10m_e c^2$, $y=(E_+-1)/(k-2)=0.9$, and the Hartree-Fock-Slater potential with the exchange term omitted.

m	0	1	2	3	4
1	0.739	0.350	-0.042	-0.414	-0.749
2	0.156	-0.050	-0.148	-0.136	-0.031
3	0.032	-0.009	0.002	0.036	0.062
4	0.014	0.006	0.008	0.007	0.001
5	0.008	0.004	0.002	-0.001	
6	0.007	0.005	0.004	0.003	
7	0.003	0.001			
8	0.001				

$$S = \frac{A}{4\pi(1-\beta_+\cos\theta_+)^m} \sum_{n=0}^N B_n P_n(\cos\theta_+), \quad (2)$$

where $B_0=1$ and A is defined by

$$\int S d\Omega_+ = 1. \quad (3)$$

Such representations have been used to characterize the photoelectron and electron bremsstrahlung angular distributions, and to improve the convergence of partial-wave series for elastic scattering [12]. To illustrate the improved convergence in pair-production shape function, which can be obtained with convergence factors of the type in Eq. (2), we show in Table I for $Z=82$, $K=2.10m_e c^2$, $y=(E_+-1)/(k-2)=0.9$, and the HFN potential, the coefficients B_n for $m=0-4$. We see that the best choice in this case is $m=4$, for which only

TABLE II. Coefficients B_n and A of the shape functions S in Eq. (2) with $m=4$ calculated from results of the shape functions obtained by the partial-wave method using Eqs. (21) and (23) of Ref. [4] for $Z=1,6,13,82$; $k=2.001,2.01,2.10m_e c^2$; $y=(E_+-1)/(k-2)=0.1,0.3$; and the Hartree-Fock-Slater potential with the exchange term omitted.

y	k	Z	B_1	B_2	B_3	B_4	A	
0.1	2.001	1	-0.016 14	-0.116 96	0.001 53	-0.000 04	0.999 66	
		6	0.000 50	-0.077 32	0.000 16	-0.000 01	0.999 35	
	2.01	1	-0.062 90	-0.097 86	0.003 88	0.000 51	0.997 36	
		6	-0.052 38	-0.096 71	0.003 32	-0.000 06	0.996 72	
	2.10	13	1	-0.030 89	-0.091 04	0.002 11	0.000 13	0.995 43
			13	-0.205 84	-0.084 44	0.012 03	0.000 06	0.975 36
82		-0.202 02	-0.068 46	0.010 25	0.000 03	0.974 22		
0.3	2.001	1	-0.031 00	-0.274 80	0.006 01	0.000 23	0.999 23	
		6	-0.021 77	-0.111 16	0.001 45	0.000 03	0.998 80	
	2.01	1	-0.102 25	-0.286 26	0.019 39	-0.000 13	0.992 93	
		6	-0.104 98	-0.195 54	0.013 31	-0.000 03	0.992 49	
	2.10	13	1	-0.098 77	-0.131 07	0.008 00	0.000 17	0.991 32
			13	-0.322 25	-0.267 18	0.062 41	0.000 30	0.933 93
		82	-0.359 56	-0.147 99	0.040 74	0.000 29	0.937 20	
				-0.404 19	-0.117 50	0.034 91	0.001 87	0.950 00

TABLE III. Same as Table II, except for $y = (E_+ - 1)/(k - 2) = 0.5, 0.7, 0.9$.

y	k	Z	B_1	B_2	B_3	B_4	A
0.5	2.001	1	-0.038 78	-0.431 72	0.011 26	0.000 37	0.998 87
		6	-0.035 05	-0.137 24	0.002 80	0.000 05	0.998 33
	2.01	1	-0.119 83	-0.479 84	0.043 31	0.001 60	0.989 25
		6	-0.137 07	-0.291 65	0.025 76	0.000 04	0.989 05
	2.10	13	-0.140 60	-0.163 78	0.014 19	0.000 20	0.987 83
		1	-0.368 90	-0.464 67	0.131 63	0.000 37	0.901 50
		13	-0.443 60	-0.249 72	0.084 74	0.000 29	0.907 23
	2.10	82	-0.552 01	-0.090 07	0.047 38	0.001 29	0.936 37
		2.001	1	-0.042 68	-0.588 09	0.021 22	0.000 48
6			-0.045 53	-0.161 44	0.004 23	0.000 01	0.997 91
2.01	1	-0.129 62	-0.679 47	0.071 90	-0.005 17	0.986 66	
	6	-0.159 46	-0.391 29	0.041 69	0.000 33	0.986 19	
	13	-0.172 52	-0.195 82	0.020 95	0.000 29	0.984 66	
2.10	1	-0.379 24	-0.673 50	0.213 42	-0.000 37	0.876 95	
	13	-0.488 94	-0.379 67	0.142 48	0.000 11	0.884 13	
	82	-0.661 60	-0.060 14	0.055 86	0.000 85	0.923 98	
0.9	2.001	1	-0.045 77	-0.748 59	0.028 14	0.000 11	0.998 39
		6	-0.054 09	-0.184 49	0.005 83	0.000 06	0.997 51
	2.01	1	-0.130 44	-0.877 02	0.105 30	-0.000 78	0.984 79
		6	-0.175 36	-0.496 67	0.060 13	0.000 14	0.983 91
	2.10	13	-0.198 91	-0.228 42	0.028 33	0.000 35	0.981 78
		1	-0.364 83	-0.888 25	0.300 93	0.001 52	0.859 29
		13	-0.504 25	-0.542 52	0.214 93	-0.000 26	0.868 52
	2.10	82	-0.749 19	-0.030 63	0.061 89	0.000 66	0.912 47

B_1, B_2, B_3, B_4 are needed to characterize the shape function S . This is also the best choice for the cases we consider in this paper. In Tables II and III we present the coefficients B_n and A of the shape function S in Eq. (2), with $m=4$ calculated from results of the shape functions

obtained by the partial-wave method using Eqs. (21) and (23) of Ref. [4] for the cases we consider. With the shape functions, we need the pair-production energy spectrum $\sigma(E_+)$ to determine the pair-production positron energy-angle cross section $\sigma(E_+, \theta_+)$. In Table IV we

TABLE IV. Unpolarized pair-production cross section $\sigma(E_+) = [Z^{-2} d\sigma/dE_+]_{\text{unpol}}$ for $k=2.001, 2.01, 2.10 m_e c^2$; $Z=1, 6, 13, 82$; $y=(E_+ - 1)/(k - 2) = 0.1, 0.3, 0.5, 0.7, 0.9$; calculated with the partial-wave method using Eq. (21) of Ref. [4] for the Hartree-Fock-Slater potential with the exchange term omitted (σ_{HFN}). Here the cross section σ_{HFN} is in the unit of $\mu b/m_e c^2$, and $a[n]$ shall mean $a \times 10^n$.

Z_y	k	0.1	0.3	0.5	0.7	0.9
2.001	1	5.133[-5]	1.494[-4]	2.171[-4]	2.574[-4]	2.743[-4]
	6	1.048[-5]	1.055[-4]	3.058[-4]	5.933[-4]	9.509[-4]
2.01	1	0.008 331	0.016 13	0.019 27	0.019 24	0.015 31
	6	0.002 539	0.013 55	0.024 80	0.034 56	0.043 62
	13	6.890[-4]	0.008 461	0.024 08	0.044 78	0.068 45
2.10	1	0.927 9	1.517	1.693	1.584	1.101
	13	0.318 4	1.318	2.001	2.353	2.470
	82	0.001 108	0.107 9	0.704 3	2.115	4.420

give the unpolarized pair-production positron energy spectrum for $k=2.001, 2.01, \text{ and } 2.10m_e c^2$; $Z=1, 6, 13, 82$; $y=(E_+-1)/(k-2)=0.1, 0.3, 0.5, 0.7, 0.9$, calculated with the partial-wave method using Eq. (21) of Ref. [4] for the Hartree-Fock-Slater potential with the exchange term omitted (denoted as σ_{HFN}) [13].

ACKNOWLEDGMENT

This work was supported in part by the National Science Council, Republic of China, under Grant No. NSC 83-0208-M-008-026.

-
- [1] I. Øverbø, K. J. Mork, and H. A. Olsen, *Phys. Rev.* **175**, 1978 (1968); *Phys. Rev. A* **8**, 668 (1973); I. Øverbø, Ph.D. thesis, University of Trondheim, 1970 (unpublished); J. W. Motz, H. A. Olsen, and H. W. Koch, *Rev. Mod. Phys.* **41**, 581 (1969).
- [2] H. K. Tseng and R. H. Pratt, *Phys. Rev. A* **4**, 1835 (1971); **6**, 2049 (1972).
- [3] H. K. Tseng and R. H. Pratt, *Phys. Rev. A* **21**, 454 (1980); **24**, 1127 (1981).
- [4] H. K. Tseng, *Phys. Rev. A* **50**, 343 (1994). Unrationalized units are used throughout, i.e., $\hbar=m_e=c=1$, unless otherwise specified. There are several misprints in this reference. The l_2 in Eq. (23) of this reference should be replaced by l_1 , and the \hat{p}_1 in Eqs. (26) and (27) should be replaced by $(-\hat{p}_1)$.
- [5] J. H. Hubbell, H. A. Gimm, and I. Øverbø, *J. Phys. Chem. Ref. Data* **9**, 1023 (1980); H. E. Johns and J. R. Cunningham, *The Physics of Radiology* (Thomas, Springfield, IL, 1983); F. Bagne, *Med. Phys.* **7**, 664 (1980).
- [6] R. H. Pratt, in *Fundamental Processes in Energetic Atomic Collisions*, edited by H. O. Lutz, J. S. Briggs, and H. Kleinpoppen (Plenum, New York, 1983), p. 150.
- [7] D. A. Liberman, D. T. Cromer, and J. T. Waber, *Comput. Phys. Commun.* **2**, 107 (1971).
- [8] W. Kohn and L. S. Sham, *Phys. Rev.* **140**, A1133 (1965).
- [9] R. L. Gluckstern and M. H. Hull, Jr., *Phys. Rev.* **90**, 1030 (1953); H. A. Bethe and W. Heitler, *Proc. R. Soc. London Ser. A* **146**, 83 (1934).
- [10] Y. Nishina, S. Tomonaga, and S. Sakata, *Sci. Pap. Inst. Chem. Res. Suppl. Tokyo* **24**, 17 (1934).
- [11] There is an error in the result presented in our previous work (Ref. [4]) for $Z=6$, $k=2.001m_e c^2$, and $y=0.1$. The result shown in this paper has been corrected.
- [12] H. K. Tseng, R. H. Pratt, Simon Yu, and A. Ron, *Phys. Rev. A* **17**, 1061 (1978); H. K. Tseng, R. H. Pratt, and C. M. Lee, *ibid.* **19**, 187 (1979); D. G. Ravenhall and R. N. Wilson, *Phys. Rev.* **95**, 500 (1954); S. R. Lin, *ibid.* **133**, A965 (1964).
- [13] Unfortunately, there are no experimental results available for unpolarized pair-production cross sections $\sigma(E_+)$ and $\sigma(E_+, \theta_+)$ at these low-energy cases to make comparisons with our calculated results. The status of experimental work on the pair-production cross section to 1981 has been summarized by Motz, Olsen, and Koch (see Ref. [1]), Øverbø, Mork, and Olsen (see Ref. [1]), Tseng and Pratt (see Refs. [2,3]), and F. T. Avignone III and Ali E. Khalil, *Phys. Rev. A* **24**, 2920 (1981).